Nonuniform Distribution of Short Branches in Two-Dimensional Simulations of the Amorphous Regions between Two Crystalline Lamellae

Saubhagya C. Mathur and Wayne L. Mattice*

Department of Polymer Science, The University of Akron, Akron, Ohio 44325.
Received August 11, 1987

ABSTRACT: The amorphous regions between two crystalline lamellae for chains containing approximately 6 and 11 short branches per 1000 bonds have been simulated on a square lattice with all sites occupied. The probability for the formation of a tie is not a monotonic function of branch content when the branches occupy two lattice sites. Tight folds increase and adjacent reentry (other than tight folds) decreases upon the incorporation of branches. Branches that occupy two lattice sites are not distributed randomly throughout the amorphous region; they tend to segregate near the crystal-amorphous boundary. The importance of the crystal-amorphous interface in affecting the conformations of chains in the amorphous regions is more apparent in the presence of branches that occupy two lattice sites than in the presence of shorter branches.

Introduction

The importance of copolymers of ethylene with a small amount of a 1-alkene, which are known by the common name linear low-density polyethylene, is well established. Great interest in these copolymers is due to the range of properties achievable by the selection of the type and amount of 1-alkene used as the comonomer in the polymerization. The short branches present are of uniform structure because they arise from the 1-alkene comonomer. In contrast, the material obtained upon the free radical initiated polymerization of ethylene at high pressure contains both short and long branches, with the short branches being of nonuniform structure.[1,2] The copolymers have greater tensile strength and tear strength than the conventional high- or low-pressure polyethylenes. Their properties cannot be obtained with blends of conventional high- and low-pressure polyethylene.[3,4]

Methyl branches can be accommodated in the crystalline regions of polyethylene.[5-10] However, studies[10,11] of hydrogenated polybutadiene and several ethylene-1-alkene copolymers show that close packing of the chain segments in the crystallites requires exclusion from the crystalline regions of short branches larger than methyl. A rational explanation of the dependence of the properties on the type and amount of branch content therefore requires characterization of the conformational properties of chain segments that lie in the amorphous regions between crystalline lamellae.

The problem can be attacked by two methods that differ in their attention to intramolecular and intermolecular interactions. The simpler method involves the combination of the characteristic ratio for the branched chains with the analytical models based on the Gambler's ruin problem.[12-14] The characteristic ratio is defined as $\langle r^2\rangle_0/nl^2$, where $\langle r^2\rangle_0$ denotes the mean-square unperturbed end-to-end distance for a chain with n bonds of length l in the backbone. The short-range intrachain interactions are treated in detail, but there is no special treatment of the intermolecular interactions in the interfacial region. There is also the implication that short branches are uniformly distributed throughout the amorphous region. This approach predicts that incorporation of short branches is accompanied by a decrease in the probability for formation of a tie.[15] The size of the decrease becomes unrelated to the size of the short branch when the branches are larger than ethyl. The probability for a tight fold increases with an increase in branch size and content. The increase shows no sign of a plateau even for short branches as large as octyl.[15]

The last few years have seen great interest in the simulation of lattice chains that are packed at bulk densities.[16-21] Such simulations give a less realistic account of the actual bond angles, dihedral angles, and short-range intramolecular interactions, but they can provide information about conformational effects that arise from intermolecular interactions in the interfacial region. This procedure provides the opportunity for study of the interface and the distribution of the short branches throughout the amorphous regions. Here we describe the extension of the methods used for unbranched lattice chains to the case where some of the chains bear short branches. This extension requires the imposition of new restrictions on the types of moves allowed for unbranched chains and also the development of new types of moves for the short branches. These movement rules are then applied to the simulation of amorphous branched chains packed at bulk density on a square lattice.

Simulation

Mansfield developed a method for simulating the behavior of flexible unbranched chains that are packed on a three-dimensional lattice so that there are no vacant lattice sites.[22] The method was used to study the conformational properties of unbranched chains in the amorphous region between two crystalline lamellae.[23] The bond flip described by Mansfield (with some added restrictions) is adequate for rearrangement of the main chains in the branched chains of current interest, but it cannot handle the short branches in the present system. When some of the chains contain short branches of a specified type and specified amount, the original procedure developed by Mansfield must be modified. These modifications are described below.

A. Rearrangement Moves. a. Bond Flip. Figure 1 shows the schematic representation of bond flip moves that are allowed and disallowed on a square lattice. Rearrangement may occur when parallel bonds are found on neighboring chains. Figure 1A shows this movement, which involves the simultaneous destruction and formation of two bonds. Figure 1B shows an example of a bond flip that would lead to the formation of a cyclic product. This kind of move is disallowed by the requirement that the two parallel bonds to be flipped must not belong to the same chain. Mansfield's treatment of unbranched chains allows the rearrangement in Figure 1A and prohibits the rearrangement in Figure 1B. Figure 1C shows that there must be an additional restriction on the bond flip if short branches of a *specified* size are present. Conservation of

0024-9297/88/2221-1354$01.50/0

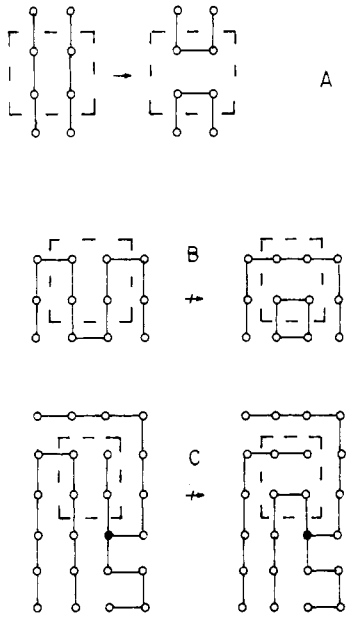

Figure 1. Bond flip moves: (A) allowed move; (B) and (C) disallowed moves. The filled circle denotes the trifunctional branch point in (C). The dashed rectangle contains the beads involved in the bond flip.

the size of the short branches demands that the bond flip may not use a bond that belongs to a short branch.

b. Branch Movements. Branch movement should permit free movement of the branches throughout the lattice while conserving the number and size of the short branches. This process does not imply that branches actually move throughout the amorphous region in a real sample by the same movement rules. Instead the movement rules prevent a bias in the lattice model that might artificially constrain the branches to certain lattice sites or artificially prevent their access to other lattice sites. The simplest possible rearrangement involving branches is similar to the "end attack" suggested by Mansfield.[22] Figure 2 shows a few examples of this movement for branches with $n_b = 1$ and 2, where n_b denotes the number of lattice sites in a branch. The movement involves destruction of the original junction of the branch with the main chain and then formation of a new attachment of the branch to a different lattice site. The chosen site may not belong to another branch because there would then be a change in the number and sizes of the short branches, as shown in Figure 2C. The end attack procedure does not meet all the criteria required for branch movement. The branches cannot freely move throughout the lattice because the lattice sites that constitute the branch are stationary. The only motion is in the lattice site that defines the trifunctional branch point. Even this motion is restricted. The trifunctional branch point may visit only four or six lattice sites respectively in parts A and B of Figure 2.

A procedure of simultaneous creation and destruction was developed to provide free movement of the branches. Figure 3A shows an example of such a movement for a branch with $n_b = 1$. A branch occupying site B1 is destroyed and a branch is created at site B2. In the process, bonds 1 and 2 are broken and reformed as bonds 3 and 4. Both the trifunctional branch point and the branch itself have changed their positions in the lattice. The branch move depicted in Figure 3A produces pathological behavior when there are four or more branches with $n_b = 1$. It permits the formation of a cluster of four branches in which the branch ends occupy a 2 × 2 section of the lattice. However, it does not provide a mechanism for

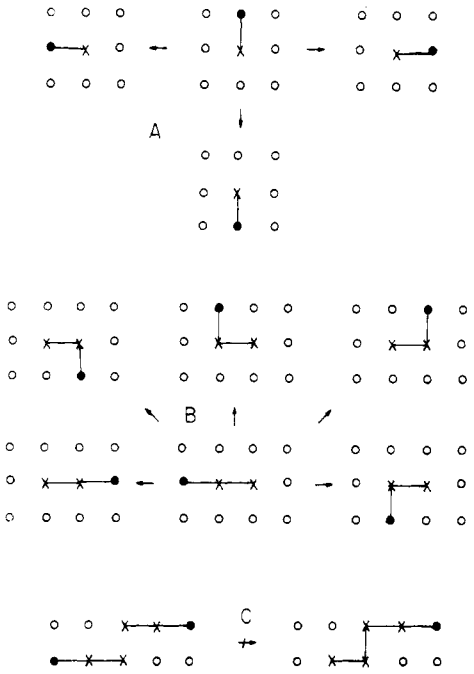

Figure 2. End attack moves involving branches that occupy one or two lattice sites. The lattice sites that constitute the branches are depicted by ×, the site that constitutes the trifunctional branch point is denoted by a filled circle, and open circles denote lattice sites that are neither branches nor trifunctional branch points.

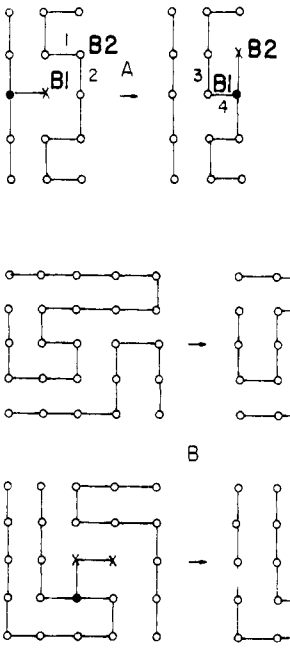

Figure 3. Simultaneous creation and destruction of branches that occupy (A) one and (B) two lattice sites.

disruption of this cluster. In practice, useful simulations can be performed when a 30 × 30 lattice contains as many as 10 branches with $n_b = 1$. The properties of interest attain constant values long before there is the irreversible formation of a 2 × 2 cluster of branch ends. On the other hand, no useful results are obtained on the same lattice in the presence of 20 branches with $n_b = 1$. The irreversible formation of 2 × 2 clusters can be detected before there is stabilization of the properties of interest.

Figure 3B shows an example of the movement used when $n_b = 2$. Here the movement is more complicated. This figure depicts changes that are performed simultaneously in independent regions of the lattice. The move illustrated in the top portion of Figure 3B breaks two

bonds, forms two new bonds, and creates a branch. The simultaneous move illustrated in the bottom portion breaks two bonds, forms two bonds, and destroys a branch. There is no correlation between the vertical/horizontal orientation of the new and old branches because the coupled moves take place in independent regions of the lattice.

B. Algorithm. Initially all chains and branches are laid out in a regular array on the lattice, making sure that there are no vacant lattice sites. At the beginning of a move cycle, one of the beads in the lattice is randomly selected. If the bead selected is on a branch, then end attack (e.g., A or B of Figure 2) is attempted. If the bead does not belong to a branch, then another bead is selected from the four coordinating beads. The bonds connected to the beads are located and a bond flip (e.g., Figure 1A) is attempted. In the next step a branch is selected at random and simultaneous creation and destruction of a branch is attempted (e.g., A or B of Figure 3). The algorithm then returns to the beginning of the move cycle until the desired number of moves has been attempted.

Periodic boundary conditions are used in the directions perpendicular to the normal to the crystal–amorphous boundary. Initially the system is taken through several rearrangement moves and the various quantities of interest are obtained. Now the rearranged system is again taken through several sets of such rearrangements. After each set, the parameters of interest are evaluated and the averaging is done over a number of such sets until the values stabilize.

C. Choice of Lattice Size and Parameters of Interest. Two factors must be considered in choosing an optimum lattice size in terms of the separation between the two layers which form the crystal–amorphous boundary. The first one is the possibility of identifying an interfacial region and the second one is the computer time required for simulation. An isotropic region distinct from the interfacial region will not be detected if the lattice is too small. On the other hand, the upper limit for the size will be governed by the computer time required for simulation. A square lattice of size 30 × 30, containing 900 beads and 30 chains, was found to be optimum from this point of view. Simulations were performed with $n_b = 0$, 1, and 2, with the number of branches being 10 when $n_b = 1$ and 5 or 10 when $n_b = 2$. This combination provides a system without branches as a reference point. Branches of two sizes are also used. The simulations performed permit comparison of results when $n_b = 1$ and 2 and (a) the number of branches is 10 or (b) the number of lattice sites in branches is 10.

The parameters of interest in this study are the probabilities of ties (obtained in terms of fraction of chains that are ties), loops, tight folds, and adjacent reentry. These conformations are shown in Figure 4, which depicts the schematic representation of the lattice. Branch distribution, in terms of the fraction of sites in each layer which are trifunctional branch points and branch ends, was also evaluated. Each layer was also studied for the various possible types of bond connections shown in Figure 5 and fraction of beads belonging to tie chains. All allowed lattice configurations are of the same energy. There is no intramolecular short-range discrimination between the bond connections depicted in Figure 5. We therefore ignore the discrimination between t and g placements, and between g^+g^+ and g^+g^- pairs, that is present in polyethylene.[24] This intentional neglect of the energetics of short-range interactions can be justified because the major interest is in the comparison of simulations without short branches and with short branches of different types when all simulations employ the same energetics.

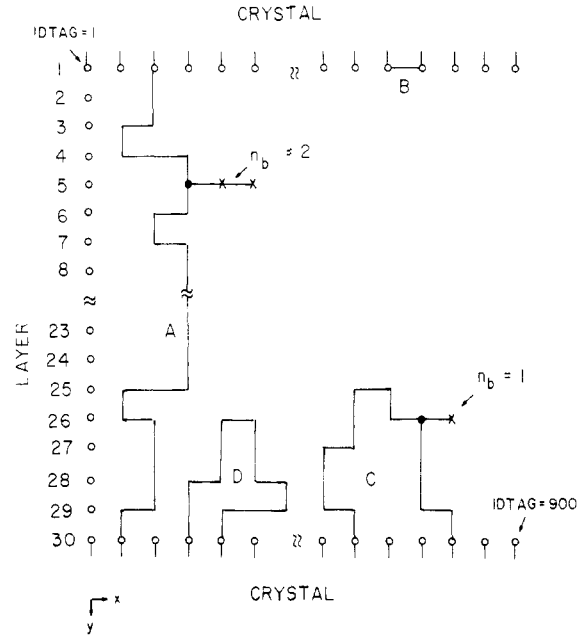

Figure 4. Schematic representation of the lattice: (A) tie; (B) tight fold; (C) loop; (D) adjacent reentry.

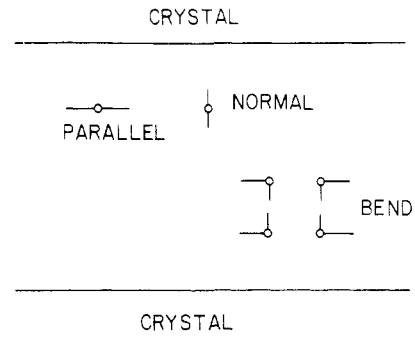

Figure 5. Various types of consecutive bonds: normal, where two successive bonds are normal to the crystal–amorphous boundary; bend, two successive bonds are perpendicular to each other; parallel, two successive bonds are parallel to the crystal–amorphous boundary.

D. Computational Details. Each lattice site (bead) was identified by an IDTAG which was a positive integer calculated from the coordinate of the bead as $Lx + y + 1$, where $L = 30$ for the present case. The layers in the lattice were sequentially numbered 1 through 30 as one goes from the top layer to the bottom ($y = 0$ to $y = 29$). Thus layer number 1 started with bead with IDTAG = 1 and the layer number 30 ended with bead with IDTAG = 900. The axis system chosen is shown in Figure 4. All the IDTAGs for the lattice were stored in a two-dimensional array KAR (I,J) with dimensions 30 × 30 for ease of location of any bead in the lattice. The chains were stored in another two-dimensional array IC (I,J) of IDTAGs. The columns in this array identified the particular chain and the rows identified the position of a bead in the particular chain. To allow for rearrangements which result in change in the number of beads in the chains, empty space (series of zeros) was alloted in each column of the array IC (I,J). The beads at the crystal–amorphous boundaries, i.e., layers 1 and 30, were separately stored in another array ICR containing 60 elements.

The regions above layer 1 and below layer 30 were assumed to be crystalline. A chain entering layer 1 or 30 from the crystalline regions to the amorphous region was initially normal to these layers. At layers 1 and 30 the

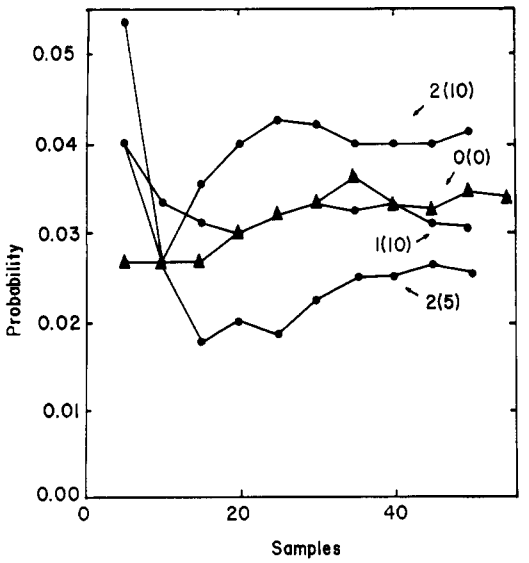

Figure 6. Variation in fraction of chains that are ties as a function of the number of sets used in the averaging. There were $\sim 10^4$ attempted moves in each set. The curves are identified by two numbers that are the values of n_b (n_{bp}).

chain can take a step normal to the layer and form a tie, loop, or adjacent reentrant loop. A chain can also take the first step parallel to layer 1 and 30 and enter the crystalline regions through the adjacent site and form a tight fold. These tight folds are the zeroth-order tight folds defined by Mansfield.[23] The chains which traverse from one boundary layer to the opposite one are the tie chains, while those that enter the crystalline region through the same boundary layer are loops (other than tight folds). Adjacent reentry is defined by chains which are loops that enter the crystalline regions through a site which is adjacent to the site from which the loop emerges. In Figure 4, chains such as A are ties, B are tight folds, C are loops, and D are the loops that belong to the category of adjacent reentry.

For the branched system, the branches are stored in a two-dimensional array of IDTAGs IBR (I,J) with dimension $(n_b + 1) \times n_{bp}$, where n_{bp} denotes the number of trifunctional branch points. The columns identify the particular branch and rows identify the position of a bead on the branch. Thus the first row has beads which are trifunctional branch points, while the last row contains beads which are branch ends.

All the rearrangement moves are thus accompanied by manipulation of the arrays of IC and IBR. After each successful move, the arrays are updated. The zero elements in IC are replaced by IDTAGs of the beads which become part of the chain and the elements corresponding to these beads in the other chain are replaced by zeros. Counting the nonzero elements in IC gives the number of beads in a particular chain. A typical set of 10 000 attempted moves takes 20, 45, and 120 min of cpu for n_b = 0, 1, or 2, respectively, on main frame IBM 3090 when 10 branches are present. For generating the averages of various quantities, 50 different sets of varying size were used.

Results and Discussion

The branches that occupy one or two lattice sites should not be equated to methyl and ethyl branches due to the artificial restrictions imposed by the lattice on bond angles and dihedral angles.[25] They do illustrate the types of effects that can be expected upon a change in the size of the short branches.

Ties, Loops, and Tight Folds. Figure 6 depicts the variation in the fraction of the chains that are ties as a function of the number of sets used in the averaging. It shows that 50 samples are quite adequate as the values tend to stabilize. Simulations with n_b = 0 and 1 give nearly indistinguishable probabilities for ties. However, when n_b is two, the probability of a tie initially decreases with incorporation of a small number of branches and then increases upon incorporation of a larger number of branches. The probability of a tie is not a monotonic function of branch content or branch size. This result is different from the one previously obtained from the Gambler's ruin approach,[15] where a decrease in the probability of ties was observed upon incorporation of branches. It indicates an important influence of the crystal–amorphous boundary in two dimensions.

Table I
Fraction of the Chains That Form Ties and Various Types of Loops

n_b	n_{bp}	tie	tight fold	loop[a]	adjacent[b]
0	0	0.034	0.52	0.44	0.23
1	10	0.032	0.57	0.40	0.21
2	5	0.025	0.59	0.38	0.17
2	10	0.041	0.62	0.34	0.14

[a] Loops other than tight folds. [b] Adjacent reentrant loops other than tight folds.

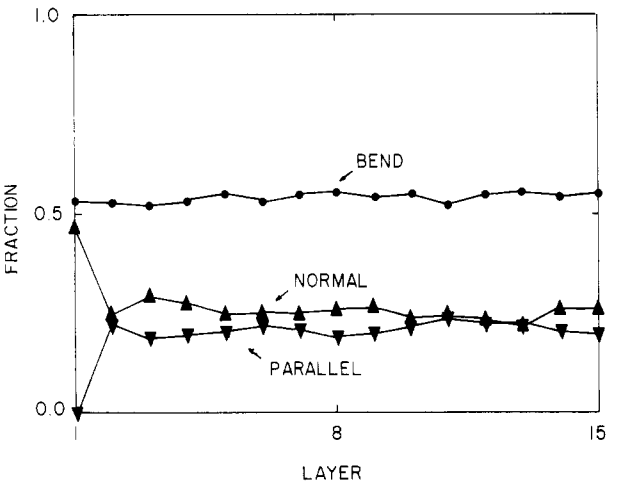

Figure 7. Variation in the different types of bond connections with distance from the crystal–amorphous boundary (layer number) for the unbranched system.

Table I summarizes the occurrence of different types of chains in the simulations. For a particular line, the sum of the entries in the third, fourth, and fifth columns is one. The final column reports the occurrence of those loops that achieve adjacent reentry by means other than the formation of a tight fold. Ten lattice sites are devoted to branches in the simulations for which results are reported on the second and third lines. Both simulations have the same volume fraction of branches in the amorphous phase. Ten lattice sites are devoted to trifunctional branch points and to branch ends, in the simulations for which results are reported on the second and fourth lines of Table I. These two simulations employ the same mole fraction of branches in the amorphous phase. Since the fractions reported on the second line of Table I are different from those on the third and fourth lines, the effectiveness of the short branches on the amorphous region is not determined exclusively by either the mole fraction or the volume fraction. When comparing simulations where n_b has the values of one and two, it is seen that the larger branch produces changes that are greater than those expected on the basis of the volume fraction or mole fraction.

Bond Pairs. Figures 7–9 show the variation of the

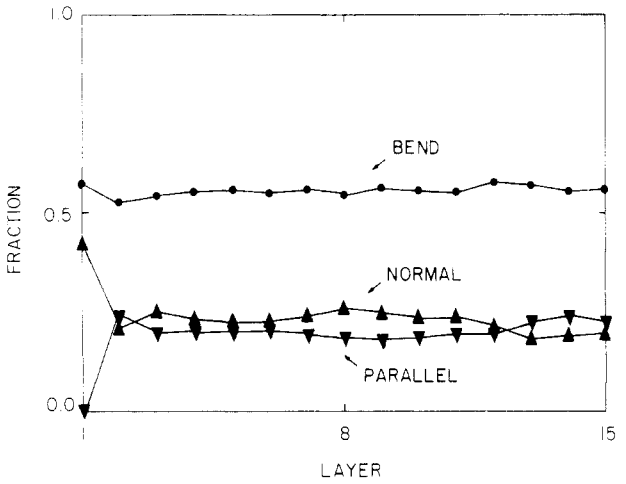

Figure 8. Same as Figure 7 for $n_b = 1$ and $n_{bp} = 10$.

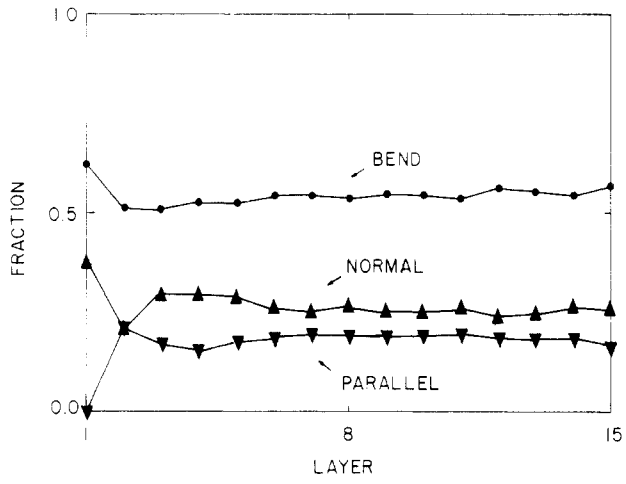

Figure 9. Same as Figures 7 and 8 for $n_b = 2$ and $n_{bp} = 10$.

fraction of different kinds of bond connections, defined in Figure 5, as a function of the layer numbers. The values have been averaged over pairs of beads in the corresponding layers equidistant from the two crystal–amorphous boundaries. Thus values at layer i correspond to the average of the value at layer i and layer $30 - (i - 1)$.

A parallel bond pair cannot occur in layer 1 because it would force a free end in the zeroth layer. The bend bond pairs at lattice sites in layer 1 arise from tight folds. The probability for tight folds, and also the probability for bend pairs in layer 1, increases from 0.52 in the absence of branches to 0.62 in the presence of branches that occupy two lattice sites. The remainder of the lattice sites in layer 1 have normal bond pairs.

Normal and parallel bond pairs occur with nearly equal probability at lattice sites in layer 2. The probability for bend bond pairs at lattice sites in layer 2 is nearly independent of the presence or absence of branches. The tendency of the short branches to increase the probability for bend bond pairs does not extend beyond layer 1.

At layers further from the crystal–amorphous interface than layer 2, the most interesting influence of the short branches is on the ratio of normal and parallel bond pairs. This ratio must be one if the region is isotropic. If the ratio is different from one, the region is under the influence of the nearby crystalline region and is therefore called an interfacial region. In the absence of branches, there is a slight suggestion that this ratio may be greater than in layer 3 and several following layers, but this tendency is no longer apparent at layer 10. On this basis, the interfacial region is quite small when branches are absent and all configurations are weighted equally. Mansfield found the interfacial region to be very small on a cubic lattice when all chain conformations were of equal energy, which is in harmony with the result obtained here with the square lattice.

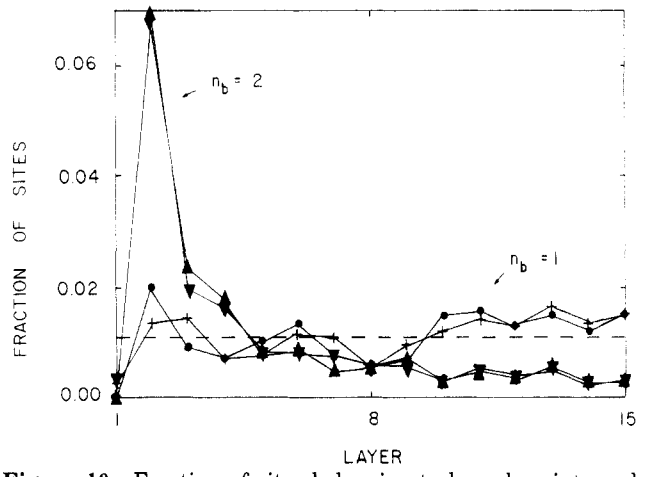

Figure 10. Fraction of sites belonging to branch points and branch ends when $n_{bp} = 10$: (+) branch point, $n_b = 1$; (▼) branch point, $n_b = 2$; (●) branch end, $n_b = 1$; (▲) branch end, $n_b = 2$. The dashed line depicts the result that would have been obtained if branches were to occupy all layers with equal probability.

Figure 9 shows that the preference for normal over parallel bond pairs persists to much higher layers in the presence of 10 branches that occupy two lattice sites. In contrast, the same number of branches that occupy a single lattice site produces no detectable elevation in the normal-to-parallel ratio, as is shown in Figure 8. If the number of branches with $n_b = 2$ is reduced to five, the behavior of the normal and parallel bond pairs in layers 3–15 is nearly indistinguishable from that depicted in Figure 7. Analysis of the Raman internal modes shows that the interfacial regions do indeed increase dramatically upon the incorporation of short branches.[9]

Distribution of Branches. The computation from the Gambler's ruin approach[15] was based on the assumption that the short branches are uniformly distributed throughout the amorphous region. However, the results from the present simulation indicate otherwise for the longer branches in the two-dimensional system. Figure 10 depicts the variation in fraction of beads that are branch points and the fraction of beads that are branch ends as a function of layer number. Branches with $n_b = 2$ segregate near the crystal–amorphous boundary, while the shorter branches show less segregation. Segregation near the crystal–amorphous boundary of the branches with $n_b = 2$ is also seen when n_{bp} is five. No segregation of the longer branches was observed within a layer, implying that the branches are randomly distributed within the layer near the crystal–amorphous boundary. Segregation of branch points and branch ends for the longer branches at the same layer indicates that these branches prefer an alignment parallel to the crystal–amorphous boundary. The calculated fraction for such branches was found to be ~0.80, while ~0.15 are oriented perpendicular to the boundary and the remaining 0.05 form a bend. For the case of the shorter branches ~0.45 are parallel and ~0.55 are perpendicular to the boundary, indicating a relatively random distribution of orientations.

The segregation near the crystal–amorphous boundary of branches that occupy two lattice sites implies that a greater number of arrangements is accessible to the chains in this lattice when the branches are near the boundary

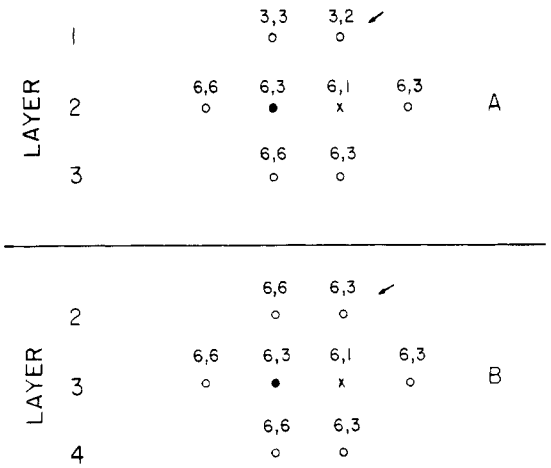

Figure 11. Beads near a branch with $n_b = 1$ when the branch is parallel to the boundary and located in layer 2 (A) or 3 (B). The branch is denoted by ×, the filled circle is the trifunctional branch point, and open circles denote nearby lattice sites that are not branches. The numbers are the possible bond pairs at the lattice site when there is no branch (left) or when the branch is present (right). The lattice sites marked by the arrows receive special attention in the text.

as compared to the case when they are randomly distributed. The significant decrease in adjacent reentrant loose loops is related to the segregation of ethyl branches (which are parallel to the crystal–amorphous boundary) near the boundary as fewer sites are available for a loop to come back and enter the crystalline region through an adjacent site. However, the fraction of tight folds is expected to increase because the chain emerging from layers below the sites occupied by a branch that occupies two sites in layer 2 must reenter the crystallite as a zeroth-order tight fold.

A qualitative rationalization of the tendency for segregation of the larger branches near the boundary can be achieved by a consideration of a product determined by the various bond pairs depicted in Figure 5. Beads at layers 2–29 may have any of the six bond pairs, but beads in layers 1 and 30 are restricted to the normal bond pair and two of the four possible bends. The product of these numbers of possible bond pairs for all beads on the 30 × 30 lattice is $3^{(2\times30)}6^{(28\times30)}$, which we denote by P. If the beads were completely independent, P would be the number of configurations of the lattice. This number greatly overestimates the number of configurations of the lattice because it neglects the correlation between beads, but it has the virtue of being easily calculated.

Now consider the effect of a single short branch on the product of possible bond pairs for all beads. Figure 11A,B depicts a branch with $n_b = 1$ that is parallel to the interface and located in layer 2 or layer 3. Two numbers are depicted above each bead. On the left is the number of bond pairs accessible to the bead when no branch is present, and on the right is the number of bond pairs accessible when the branch exists at the indicated sites. This number is taken to be one for the bead in the branch, because it can only be connected to the trifunctional branch point, and the number is three for the branch point because there are three possible ways to draw the two bonds in the main chain that involve this bead. The product of the number of possible bond pairs for the lattice is P in the absence of the branch, and it falls to $P/72$ and $P/96$ in parts A and B of Figures 11, respectively. An arrow denotes the bead responsible for the difference in results when the branch is in layer 2 or 3. The branch, bead ×, reduces the number of possible bond pairs accessible to the nearest-neighbor beads. The reduction is a factor of $^1/_2$ unless the nearest neighbor is in layer 1, in which case the factor is $^2/_3$. The ratio of these factors is $^4/_3$ and accounts for the presence of a larger product of possible bond pairs in Figure 11A than in Figure 11B.

A similar analysis of a lattice with a single branch with $n_b = 2$ that is parallel to the interface and located in layer 2 or 3 yields products of possible bond pairs of $P/1296$ and $P/2304$, respectively. The ratio is $(^4/_3)^2$ when $n_b = 2$, because of the existence of an additional bead of the type denoted by the arrow.

Consideration of the product of possible bond pairs leads to the expectation that short branches might be found more frequently in layer 2 than in layer 3, and the discrimination between layers might become more severe as the branch becomes larger. In a rudimentary fashion, the segregation of branches with $n_b = 2$, depicted in Figure 10, thereby receives a rationalization. Presumably it is the correlation between the beads that causes the ratio of these branches in layers 2 and 3 to be larger than $(^4/_3)^2$.

It is certainly worthwhile to inquire whether the segregation of branches near the boundary occurs only in two dimensions, or whether it might also be present in three dimensions. The best answer must await the results of the simulation on a cubic lattice. In the interim, one can easily extend the calculation performed above from a square lattice to a cubic lattice. For a branch with $n_b = 2$, the ratio of $(^4/_3)^2$ that was obtained with the square lattice becomes $(^6/_5)^2$ on the cubic lattice. This result suggests segregation of short branches near the interface may also be present on the cubic lattice, although it may be different in degree. The added dimension will also allow entangled loops,[26,27] which cannot occur on the square lattice.

Conclusions

Two-dimensional simulation results indicate that the presence of the crystal–amorphous boundary has a significant effect on the conformational behavior of the lightly branched chains in the amorphous region between two crystalline lamellae. The effect of the short branches is not controlled by either their mole fraction or volume fraction. Segregation near the crystal–amorphous boundary is observed for branches that occupy two lattice sites. A qualitative argument suggests that segregation may persist in three dimensions. The segregation implies that a greater number of conformations are accessible to the chains on the lattice when the branches are preferentially present near the crystal–amorphous boundary. Both the present work and the Gambler's ruin approach[15] predict an increase in tight folds upon incorporation of short branches.

Acknowledgment. This research was supported by National Science Foundation Grant DMR 86-96071 and the donors of the Petroleum Research Fund, administered by the American Chemical Society.

References and Notes

(1) Axelson, D. E.; Levy, G. C.; Mandelkern, L. *Macromolecules* **1979**, *12*, 41.
(2) Usami, T.; Takayama, S. *Macromolecules* **1984**, *17*, 1756.
(3) Clampitt, B. H. *Justus Liebigs Ann. Chem.* **1963**, *35*, 577.
(4) Datta, N. K.; Birley, A. W. *Plast. Rubber Process. Appl.* **1982**, *2*, 237.
(5) Flory, P. J. *Trans. Faraday Soc.* **1955**, *51*, 848.
(6) Swan, P. R. *J. Polym. Sci.* **1962**, *56*, 409.
(7) Richardson, M. J.; Flory, P. J.; Jackson, J. B. *Polymer* **1963**, *4*, 226.
(8) Baker, C. H.; Mandelkern, L. *Polymer* **1966**, *7*, 71.
(9) Alamo, R.; Domszy, R.; Mandelkern, L. *J. Phys. Chem.* **1984**, *88*, 6587.
(10) Voigt-Martin, I. G.; Alamo, R.; Mandelkern, L. *J. Polym. Sci., Polym. Phys. Ed.* **1986**, *24*, 1283.

(11) VanderHart, D. L.; Perez, E. *Macromolecules* **1986**, *19*, 1902.
(12) DiMarzio, E. A.; Guttman, C. M.; Hoffman, J. D. *Polymer* **1981**, *21*, 1379.
(13) Guttman, C. M.; DiMarzio, E. A.; Hoffman, J. D. *Polymer* **1982**, *22*, 1466.
(14) Guttman, C. M.; DiMarzio, E. A.; Hoffman, J. D. *Macromolecules* **1982**, *15*, 525.
(15) Mathur, S. C.; Mattice, W. L. *Macromolecules* **1987**, *20*, 2165. (In Figure 1, the scale for the vertical axis should be −0.8 to 0 instead of −6 to 0.)
(16) Dill, K. A.; Flory, P. J. *Proc. Natl. Acad. Sci. U.S.A.* **1980**, *77*, 3115.
(17) Dill, K. A.; Flory, P. J. *Proc. Natl. Acad. Sci. U.S.A.* **1981**, *78*, 676.
(18) Baumgartner, A.; Yoon, D. Y. *J. Chem. Phys.* **1983**, *79*, 521.
(19) Flory, P. J.; Yoon, D. Y.; Dill, K. A. *Macromolecules* **1984**, *17*, 862.
(20) Yoon, D. Y.; Baumgartner, A. *Macromolecules* **1984**, *17*, 2864.
(21) Boyd, R. H. *Macromolecules* **1986**, *19*, 1128.
(22) Mansfield, M. L. *J. Chem. Phys.* **1982**, *77*, 1554.
(23) Mansfield M. L. *Macromolecules* **1983**, *16*, 914.
(24) Abe, A.; Jernigan, R. L.; Flory, P. J. *J. Am. Chem. Soc.* **1966**, *88*, 631.
(25) Flory, P. J. *Proc. Natl. Acad. Sci. U.S.A.* **1982**, *79*, 4510.
(26) Lacher, R. C.; Bryant, J. L.; Howard, L. N.; Sumners, D. W. *Macromolecules* **1986**, *19*, 2639.
(27) Lacher, R. C.; Bryant, J. L.; Howard, L. N. *J. Chem Phys.* **1986**, *85*, 6147.

Block Copolymers at Interfaces. 1. Micelle Formation

Mark R. Munch and Alice P. Gast*

Department of Chemical Engineering, Stanford University, Stanford, California 94305.
Received March 17, 1987; Revised Manuscript Received October 16, 1987

ABSTRACT: We apply the theory of Leibler et al. (*J. Chem. Phys.* **1983**, *79*, 3550) to describe the micellization of diblock copolymers in solutions. First, we consider the formation of spherical micelles and find that the critical micelle concentration and aggregation number increase as the copolymer–solvent compatibility increases, as the B block becomes smaller relative to the A block, and as the size of the solvent decreases. We also show how the radius of the micelle increases as the B blocks and solvent become less compatible. We discuss some limiting cases and give approximations for the model in the limit of small critical micelle concentration. We then consider the formation of lamellar micelles and predict regimes where lamellar micellization precludes that for spheres. Lamellar micelles are favored when the B and A blocks are equal in length and the solvent size is large.

I. Introduction

The behavior of amphiphilic diblock copolymers at interfaces plays an important role in homogenization of polymer blends,[1] detergency or surfactancy, and stabilization of colloidal particles.[2] Stabilization of colloidal particles is realized by adsorption of diblock copolymers onto their surfaces. The block interacting unfavorably with the solvent adsorbs onto the surface of a particle while the solvated block extends into the solution and forms a steric layer thus imparting stability. This adsorption process is complicated by the tendency of amphiphilic block copolymers to form micelles if the concentration of the solution exceeds the critical micelle concentration, cmc. The critical micelle concentration is defined as the concentration below which virtually no micelles exist and above which all additional copolymer goes into the micellar phase.[3] Since the critical micelle concentration often occurs at very low concentrations, a model of the adsorption process must include a description of micellization. The goal of this work is to address this problem by first describing the micellization process in this paper, and then, in the following paper, extending our analysis to block copolymer adsorption.

Theoretical models have been developed employing the mean-field theory to describe cmc and size of micelles.[4–6] We follow the development of Leibler et al.[4] who present a theory for micelle formation for a mixture of diblock copolymer and homopolymers. They considered copolymers of equal block lengths with a homopolymer of degree of polymerization typically one-fifth the polymerization index of the copolymer. Roe[7] shows a reasonable comparison between the results of this theory and the experimental results of Rigby and Roe.[8,9]

The purpose of this paper is to qualitatively describe micelle formation in block copolymers with much smaller insoluble head groups and in solutions of smaller solvent molecules than those treated previously.[4–6] One motivation for focusing our attention on these systems arises from the observation that colloidal stability is improved by maximizing the number of chains on the surface.[2] We expect the surface density of adsorbed block copolymers to increase with decreasing anchoring unit size, hence we focus our attention on systems with small head groups. Another motivation for studying small head groups arises from the many studies of surfactant systems typically having very small polar head groups. Generally systems of practical importance contain a solvent whose molecular size is much smaller than the copolymer molecules', and thus we also investigate this small-solvent regime.

We briefly present the model of Leibler et al.[4] and define the important parameters of this study, the ratio of block lengths, the relative solvent size, and the solvent compatibility. We then describe results of numerical calculations showing several important trends. We demonstrate that the critical micelle concentration increases as the relative length of the less soluble block decreases, as the size of the solvent decreases, and as the solubility of the head group increases. We note an interesting result that the radius of the micelle increases when the solubility of the head group decreases even though the number of chains per micelle decreases.

We present some useful asymptotic results showing the regimes where polydispersity becomes important, invalidating the assumptions of monodisperse spherical micelles, and where the cmc, chains per micelle, and micelle size can be predicted from simple expressions. We also describe

0024-9297/88/2221-1360$01.50/0